

EFFECTIVE FORCES BETWEEN COLLOIDAL PARTICLES

Riina Tehver¹, Jayanth R. Banavar¹, ¹Department of Physics and Center for Materials Physics, Pennsylvania State University, University Park, Pennsylvania 16802, Joel Koplik², ²Benjamin Levich Institute and Department of Physics, City College of the City University of New York, New York, New York 10031

Colloidal suspensions have proven to be excellent model systems for the study of condensed matter and its phase behavior [1]. Many of the properties of colloidal suspensions can be investigated with a systematic variation of the characteristics of the systems and, in addition, the energy, length and time scales associated with them allow for experimental probing of otherwise inaccessible regimes [2, 3]. The latter property also makes colloidal systems vulnerable to external influences such as gravity. Experiments performed in micro-gravity by Chaikin and Russell have been invaluable in extracting the true behavior of the systems without an external field [3]. Weitz and Pusey (private communication) intend to use mixtures of colloidal particles with additives such as polymers to induce aggregation and form weak, tenuous, highly disordered fractal structures that would be stable in the absence of gravitational forces.

Between any two colloidal particles, there is an attractive force caused by the interactions between the fluctuating dipole moments of their constituent atoms. This van der Waals force leads to irreversible aggregation of unprotected particles and it is desirable to diminish its magnitude [4] and provide a stabilization mechanism. Common mechanisms are steric stabilization and charge stabilization [1]. For steric stabilization, colloidal particles are coated with polymers so that there is a short-range highly repulsive (nearly hard core) force between two colloidal particles when their respective polymer layers are compressed. We shall consider these types of colloidal particles later.

Charge stabilization occurs when charged surface groups on colloidal particles dissociate, ionizing the particle and emitting counterions into the solution. The standard theory of interaction in these charged colloidal suspensions is due to Derjaguin, Landau, Verwey and Overbeek (DLVO) [5] and the DLVO potential includes a non-negligible screened Coulomb repulsion

$$U_{DLVO}(r) = \frac{Z^*{}^2 e^2 \exp(-\kappa r)}{\epsilon r} \quad (1)$$

in addition to the short-range van der Waals attraction. The inverse Debye screening length, κ and the effective charge, Z^* are given by $\kappa^2 = 4\pi\rho e^2/k_B T\epsilon$, $Z^* = Z \exp(\kappa a)/(1 + \kappa a)$. Here, ϵ is the dielectric constant of

the solvent, ρ is the density of counterions, a is the radius of a colloidal ‘‘macroion’’, Z is its bare charge, k_B and T are the Boltzmann constant and temperature. The screened Coulomb potential is obtained in the mean-field linearized Poisson-Boltzmann approximation and is thus expected to have limited applicability, although the functional form of the potential with a renormalized charge has been argued to remain valid in a wider regime [6].

Indeed, the DLVO theory has been shown to explain some experimental data [7] but fails to account for others [8]. The main experimental challenges to the theory are numerous indications of a long-range attraction between colloidal particles. The latter are evident in experiments where particles are confined near a wall or in suspensions at higher densities. When two isolated particles at a low density have been considered, no attraction has been found. Hence, many-body effects might be thought to be responsible for this unexpected attractive force.

To study the role of confinement and evaluate many-body forces, we consider a system consisting of spherical colloidal macroions, a counterion density distribution $\rho(\vec{r})$ and a homogeneous solvent of a specified dielectric constant. The effective Hamiltonian for our system can be expressed as:

$$\mathcal{H} = \frac{1}{2} \sum_I M_I \dot{\vec{R}}_I^2 + \sum_{I,J < I} U(|\vec{R}_J - \vec{R}_I|) + \mathcal{F}. \quad (2)$$

M_I and \vec{R}_I are the masses and coordinates of the macroions and $U(|\vec{R}_J - \vec{R}_I|)$ is the macroion-macroion interaction energy. In the expression for the free energy of the counterions [9, 10],

$$\mathcal{F} = \int d^3\vec{r} \rho(\vec{r}) [\phi_{ext} + \frac{1}{2\epsilon} \phi_{int} + \phi_{id}(\rho) + \phi_{corr}(\rho)] \quad (3)$$

we include: the macroion-counterion and counterion-wall interaction potentials, ϕ_{ext} ; the Coulomb interactions between counterions, $\phi_{int}(\vec{r}) = \int d^3\vec{r}' \frac{\rho(\vec{r}')}{|\vec{r} - \vec{r}'|}$; ideal gas, ϕ_{id} , and correlation, ϕ_{corr} , contributions. The ideal gas term is $\phi_{id} = k_B T \log[\Lambda_B^3 \rho(\vec{r})] - 1$, where Λ_B is the de Broglie thermal wavelength and we employ the free energy of a one-component plasma [11] in evaluating ϕ_{corr} . We use pseudopotentials for macroion-counterion interactions [10] to suppress the large variation of the counterion density near a macroion core.

Given \mathcal{F} , the forces between macroions due to counterions can be evaluated using the Hellmann-Feynman theorem. The total force acting on a macroion becomes:

$$F_I = -\nabla_{\vec{R}_I} \mathcal{F}(\rho(\vec{r}), \phi_{ext}) - \nabla_{\vec{R}_I} \sum_J U(|\vec{R}_J - \vec{R}_I|). \quad (4)$$

The equilibrium counterion density, $\rho(\vec{r})$, itself can be obtained from a functional minimization: $\frac{\delta \mathcal{F}}{\delta \rho} = 0$. An efficient scheme for solving a functional minimization of this type was developed by Car and Parrinello [12] in the context of quantum-mechanical electronic properties calculations and also used by Lowen, Madden and Hansen [10] for colloidal suspensions. Expressing the counterion density in terms of a wave function $\psi(\vec{r})$, $\rho(\vec{r}) = |\psi(\vec{r})|^2$, one can consider the Fourier components of $\psi(\vec{r})$, $\psi_{\vec{k}}$, to be dynamical variables in a Lagrangian:

$$\mathcal{L} = \frac{1}{2} \sum_{\vec{k}} m_{\vec{k}} |\dot{\psi}_{\vec{k}}|^2 + \frac{1}{2} \sum_I M_I \dot{\vec{R}}_I^2 - \mathcal{F} - \sum_{I, J < I} U(|\vec{R}_J - \vec{R}_I|) \quad (5)$$

with a constraint: $\int d^3\vec{r} \rho(\vec{r}) = NZ$. N is the number of macroions. $m_{\vec{k}}$ are fictitious masses determining the time-scale of the dynamics of counterion density. We used this Lagrangian to solve the functional minimization by performing dynamical simulated annealing on $\psi_{\vec{k}}$ to obtain the minimum of \mathcal{F} for a fixed macroion configuration.

We started out with a configuration of two macroions in a periodic cubic box of length $1\mu\text{m}$ at a temperature $T = 300\text{K}$ in water, $\epsilon = 78$. The counterion density was evaluated on a 96^3 grid and the radius and charge of a macroion were $a = 100\text{nm}$ and $Z = 200e^-$ (e^- stands for the elementary charge). The forces between macroions at a series of different separations were measured. At this low packing fraction, relatively low surface charge and counterion concentration, the DLVO pair-potential between two macroions is expected to hold. We plot the DLVO prediction for the periodic system in Fig. 1. We show our density functional minimization results in the same figure as well as the force resulting from an *optimal* fitting to a pair-potential of the DLVO form. The numerical values for the inverse screening length and effective charge for the optimal fit are presented as the first set in Table 1.

In order to check the validity of pair-wise additivity that we had tacitly assumed above, we placed three colloidal particles in a unit cell with periodic boundary conditions. Maintaining our previous pseudopotential parameters, we studied the following geometries. First, we positioned the three macroions in configurations of equilateral triangles of different sizes and calculated

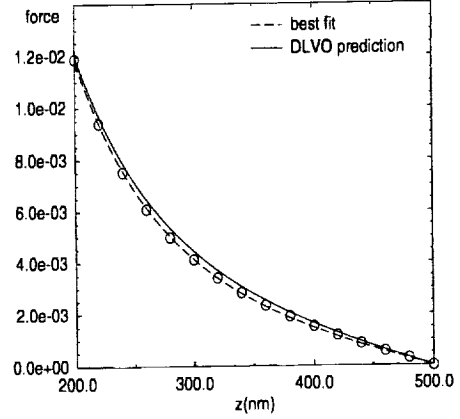


Figure 1: The total force on a macroion in a periodic system with two macroions and free counterions in the primary simulation cell. The DLVO prediction with no adjustable parameters (solid line) is compared to numerical local density approximation data (open circles) and the best fit of a DLVO-type potential is also plotted (dashed line). The force is scaled to $(e^-/nm)^2$.

the force on one of the macroions as a function of the edge of the triangle. In Fig. 2, we plot our data for the force in these configurations as a function of the distance and compare it to the force obtainable from an additive pair-potential. Secondly, we also placed the three macroions in an asymmetric triangular configuration where two macroions were close to each other (separation of 200nm) and a third macroion was at a distance of 473nm from either of the two. We measure a force of $1.24 \cdot 10^{-2} (e^-/nm)^2 \pm 0.05 \cdot 10^{-2} (e^-/nm)^2$ on either one of the first macroions while pairwise additive forces predict $1.22 \cdot 10^{-2} (e^-/nm)^2 \pm 0.05 \cdot 10^{-2} (e^-/nm)^2$ for the value. Thus, we detect no three-body component in the effective forces.

To study forces between macroions in a confined system, we introduced two parallel short-range repulsive walls. We placed the macroions at different separations and distances from a wall and measured the effective forces between them. We fit our data to a DLVO-type force and the effective parameters obtainable from the fit are summarized in Table 1. Our results can be understood as follows. The introduction of repulsive walls increased the counterion density in the middle of the simulation cell, while decreasing the Debye screening length in that region (compare sets 1 and 2 in the table). On the other hand, near the walls,

	R_x (nm)	κa	Z^* (e^-)	Z (e^-)
1	-	0.374	212.5	200.9
2	500.0	0.454	220.2	203.3
3	350.0	0.444	220.5	204.2
4	200.0	0.308	213.8	205.5

Table 1: The parameters corresponding to the optimal effective pair interaction potential between macroions in different geometries. The first set of data was obtained with periodic boundary conditions while walls were introduced in the last three. R_x measures the distance from a wall. κa and Z^* are obtained from the fit, the bare charge Z is calculated from κa and Z^* . The DLVO prediction for a periodic system is: $Z = 200$, $Z^* = 205.8$ and $\kappa a = 0.258$.

the counterion density must decrease and the Debye screening length consequently increase – the latter can be seen by comparing sets 2, 3 and 4. Thus, this simple model for confinement changes the effective parameters in the DLVO potential but does not introduce any fundamentally new behavior.

Besides electrostatic interactions, entropic depletion effects that arise from (hard-core) exclusion play an important role in determining the behavior of multicomponent colloidal suspensions [13, 14]. It is well known that the addition of free polymers to a suspension of colloidal particles can cause an effective attraction. The first successful attempt to predict and explain the phenomenon was made by Asakura and Oosawa (AO) [15]. In their approach, there is an exclusion volume around each large sphere within which the centers of small ones cannot penetrate. As the entirely entropic free energy of small spheres depends on the volume accessible to them, the favored configurations are the ones where the exclusion volumes of large spheres overlap. This implies that there ought to be a force, pushing the large spheres towards each other in order to increase the entropy of the small ones. A similar mechanism explains the attraction of a large sphere towards a wall. Quantitative AO calculations ignore the interactions between the small spheres completely and even though an overall acceptable experimental agreement with the AO prediction has been reported [13, 16], the ideal gas approximation based AO theory does not provide a satisfactory description of entropic potentials and forces in dense colloidal suspensions.

To go beyond the simple geometric arguments of AO requires a detailed theory for the structure of a binary

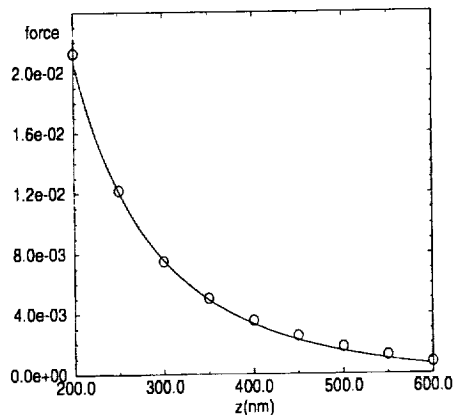


Figure 2: Test of the additivity of the effective macroion potential. Three macroions were placed in equilateral triangular configurations and the force on a macroion as a function of the edge of the triangle was measured. Open circles are our data whereas the solid line indicates the force from an additive DLVO-type potential with the parameters: $Z^* = 212.5e^-$, $\kappa a = 0.374$. The force is scaled to $(e^-/nm)^2$.

fluid. Even though significant progress has been made [17], this is a difficult task for an arbitrary binary system. We consider instead the simplest situation in which all the spheres are of the same size and study depletion forces and potentials by an analysis of the data for this system. All our numerical data were obtained from hard-sphere molecular dynamics simulations where the system evolves on a collision-to-collision basis: all particles move freely until two of them come in contact, then an elastic collision between the two occurs, after which all particles move freely until the next collision. Desired quantities are measured as equilibrium time averages in these simulations.

Let us first consider the depletion potential between two hard spheres in a “solution” of other hard spheres of the same size. The potential of mean force, W , is related to the pair correlation function, $g(x)$, as [18]

$$g(x) = \exp(-W/k_B T). \quad (6)$$

The depletion force therefore turns out to be:

$$F/k_B T = \frac{\partial \ln(g(x))}{\partial x}, \quad (7)$$

where x is the distance between two particles. An example of the depletion force between two hard spheres

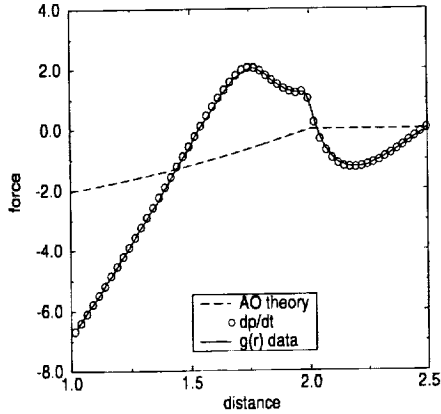


Figure 3: The depletion force as a function of the distance between two hard spheres in a mixture of other hard spheres of the same size at a packing fraction $\phi = 0.45$. The distance is measured in hard sphere diameters, σ , and the force is scaled to $k_B T/\sigma$.

in a hard-sphere fluid derived from a pair-correlation function using Eq. (7) is given in Figure 3. At a packing fraction of $\phi = 0.45$, it suffices to consider 108 hard spheres in a cubic box with periodic boundary conditions to obtain the first features in the force profile. We can prove the validity of our calculation by measuring the depletion force directly by recording the total momentum transfer in a unit time on a sphere at a known distance from another one. We compare both of those force measurements to the AO prediction in Figure 3.

Similarly, the depletion force between a sphere and a wall can be obtained from the density profile:

$$F/k_B T = \frac{\partial \ln(\rho(x))}{\partial x} \quad (8)$$

where x is the direction perpendicular to the wall and $\rho(x)$ is the local density of the hard sphere fluid. The well-known layering of fluid molecules near a wall leads again to a more complex structure for the force than AO predicts. See Fig. 4 for the force data and the AO prediction. We also plot the force obtained from momentum transfer measurements. The data was obtained with the same number of spheres at the same density as before.

Depletion forces in complex geometries with step edges and non-trivial curvature have been measured and argued to have profound consequences for cellular biology or entropic control and directed motion of colloidal particles. The AO-type calculations of entropic forces

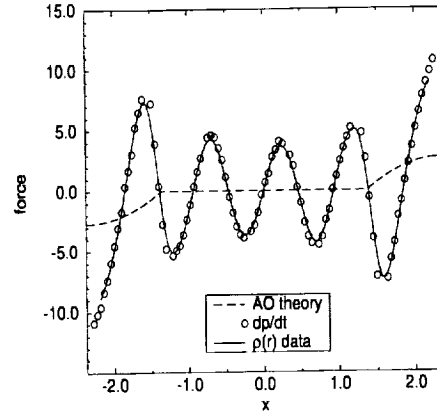


Figure 4: The depletion force between a hard sphere and a wall for the system described in the text. x is measured in hard sphere diameters and the force is scaled to $k_B T/\sigma$. The walls are parallel to the yz plane and are located at $x = \pm 2.37$. In the simulation, presented in this figure, thermal walls were used but reflecting walls result in a qualitatively similar force profile.

and potentials in these geometries are simple enough to carry out while more precise predictions quickly become rather laborious and, to our knowledge, have not been attempted. To go beyond the AO theory, we calculated entropic forces and potentials for a system of 324 hard spheres at a packing fraction of about 0.45 in a three-dimensional T-shaped channel. Potentials near step-edges and corners are of principal interest and are shown in Figure 5. A comparison with the AO prediction is also shown in the figure. The potential barrier repelling a hard sphere from a step-edge is simply a reflection of the density decrease near it. Analogously, the potential minimum attracting particles towards a corner and the sharp increase in density there are different manifestations of the same effect.

There is an interesting and important feature to the depletion forces that already manifests itself in the AO approach. Depletion forces need not be pairwise additive. In the AO approximation, the force between two particles arises from the overlap of excluded volumes. Three-body effects become relevant when the hard spheres are considered in configurations in which their pairwise overlap volumes themselves overlap, resulting in an over-counting of the actual overlap volume. An example could be a triangular configuration. The AO prediction for an equilateral configuration is calculable.

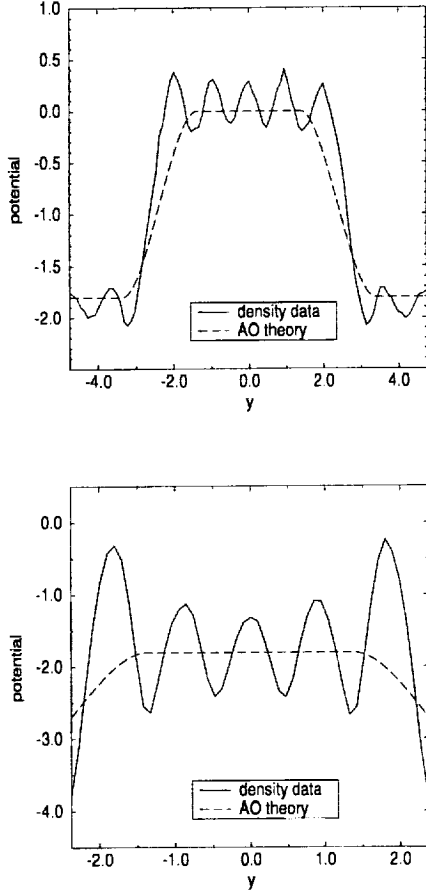


Figure 5: The effective potential profiles for a hard sphere fluid confined in a T-shaped channel. To form the channel, walls in the yz plane were placed at: $x = 4.74\sigma$; $x = 0$ for $|y| > 2.37\sigma$; $x = -4.74\sigma$ for $|y| < 2.37\sigma$; and in the xz plane at $y = \pm 2.37\sigma$ for $-4.74\sigma < x < 0$. (Periodic boundary conditions were used otherwise.) The upper figure displays the effective potential at $x = 0$, i. e. along a “step,” the edges of which are located at $y = \pm 2.37\sigma$. The lower figure is the effective potential at $x = -4.74\sigma$ where the “corners” are located at $y = \pm 2.37\sigma$. The potential is given in units of thermal energy and y is measured in hard sphere diameters.

For the packing fraction $\phi = 0.45$, the AO two-body force at two sphere contact is $F_{AO} = -2.0 k_B T/\sigma$. If forces were additive, the magnitude of the total force on a sphere in this triangular configuration would be $2F_{AO} \cos(\pi/6) = -3.5 k_B T/\sigma$. Instead, when all overlap volumes are correctly accounted for, an AO-like analysis predicts instead a force of $-2.9 k_B T/\sigma$. The *exact* three-body force can in principle be found from a three-point correlation function but obtaining reliable statistics for this measurement is rather time consuming. Instead, we prepared the described triangular configuration and measured the momentum transfer on each of the spheres in a simulation. The two-body force at contact for $\phi = 0.45$ is $F_{sim} = -6.8 k_B T/\sigma$ (see Fig. 3). The actual measured force, $-10.0 k_B T/\sigma$, is again significantly lower than the additive pairwise force: $2F_{sim} \cos(\pi/6) = -11.8 k_B T/\sigma$. Indeed, the three-body component in this geometry for our system of hard spheres is a significant percentage of the total force.

In conclusion, we have performed calculations of effective forces between charged colloidal particles in different configurations and studied effective depletion forces in hard sphere colloids. In the first case, our data are well fit to screened Coulomb type potentials. It should be noted that in our calculations, the walls were not charged and dielectric discontinuities between the suspension and the walls were not considered. One may speculate that long-range attraction cannot be accounted for by static calculations and that they probably originate from temporal fluctuations. In the second case, a comparison of our numerical data and the Asakura-Oosawa theory indicates that the AO theory underestimates the magnitude of depletion forces at contact, ignores the complex nature of entropic interactions, consisting of several maxima and minima and underestimates the range of the interactions.

Acknowledgment: This work was done in close collaboration with Francesco Ancilotto, Amos Maritan and Flavio Toigo to whom we are grateful. We are indebted to Paul Chaikin and Dave Weitz for numerous stimulating discussions and the NASA Microgravity Program for their generous support.

REFERENCES

References

- [1] P. N. Pusey, in: *Liquids, Freezing and the Glass Transition*, eds. J. P. Hansen, D. Levesque and J. Zinn-Justin (North-Holland, Amsterdam, 1991). W. C. K. Poon and P. N. Pusey, in: *Observation, Prediction and Simulation of Phase Transitions in Complex Fluids*, eds. M. Baus, L. F. Rull and J.-P. Ryckaert (Kluwer Academic, Dordrecht, 1995).
- [2] W. van Meegen and S. M. Underwood, *Nature* (London), 362, 616 (1993). K. Schatzel and B. J. Ackerson, *Phys. Rev. Lett.* 68, 337 (1992). B. J. Ackerson and P. N. Pusey, *Phys. Rev. Lett.* 61, 1033 (1988).
- [3] J. Zhu, M. Li, R. Rogers, W. Meyer, R. H. Ottewill, STS-73 Space Shuttle Crew, W. B. Russell and P. M. Chaikin, *Nature* (London), 387, 883 (1997).
- [4] The magnitude of van der Waals forces can be reduced by index matching the solvent and the particles but this is unfortunately incompatible with density matching. A micro-gravity environment is thus essential to avoid sedimentation and resulting complications.
- [5] B. V. Derjaguin and L. D. Landau, *Acta Physicochim. USSR* 14, 633 (1941). E. J. W. Verwey and J. T. G. Overbeek, *Theory of the Stability of Lyophobic Colloids* (Elsevier, Amsterdam, 1948).
- [6] S. Alexander, P. M. Chaikin, P. Grant, G. J. Morales, P. Pincus and D. Hone, *J. Chem. Phys.* 80, 5776 (1984).
- [7] J. C. Crocker and D. G. Grier, *Phys. Rev. Lett.* 73, 352 (1994).
- [8] J. C. Crocker and D. G. Grier, *Phys. Rev. Lett.* 77, 1897 (1996). A. E. Larsen and D. G. Grier, *Nature* (London), 385, 230 (1997). A. E. Larsen and D. G. Grier, *Phys. Rev. Lett.* 76, 3862 (1996). B. V. R. Tata, M. Rajalakshmi and A. K. Arora, *Phys. Rev. Lett.* 69, 3778 (1992). B. V. R. Tata and N. Ise, *Phys. Rev. B* 54, 6050 (1996). B. V. R. Tata, E. Yamahara, P. V. Rajamani and N. Ise, *Phys. Rev. Lett.* 78, 2660 (1997). K. Ito, H. Yoshida and N. Ise, *Science* 263, 66 (1994).
- [9] M. J. Stevens and M. O. Robbins, *Europhys. Lett.* 12, 81 (1990).
- [10] H. Lowen, P. A. Madden and J.-P. Hansen, *Phys. Rev. Lett.* 68, 1081 (1992). H. Lowen, J.-P. Hansen and P. A. Madden, *J. Chem. Phys.* 98, 3275 (1993).
- [11] M. Baus and J.-P. Hansen, *Phys. Rep.* 59, 1 (1980).
- [12] R. Car and M. Parrinello, *Phys. Rev. Lett.* 55, 2471 (1985).
- [13] A. D. Dinsmore, A. G. Yodh and D. J. Pine, *Nature* (London) 383, 239 (1996). A. D. Dinsmore, D. T. Wong, P. Nelson and A. G. Yodh, *Phys. Rev. Lett.* 80, 409 (1998).
- [14] P. D. Kaplan, J. L. Rouke, A. G. Yodh and D. J. Pine, *Phys. Rev. Lett.* 72, 582 (1994). P. D. Kaplan, L. P. Faucheux and A. J. Libchaber, *Phys. Rev. Lett.* 73, 2793 (1994). A. Imhof and J. K. G. Dhont, *Phys. Rev. Lett.* 75, 1662 (1995). P. Bartlett, R. H. Ottewill and P. N. Pusey, *Phys. Rev. Lett.* 68, 3801 (1992).
- [15] S. Asakura and F. Oosawa, *J. Chem. Phys.* 22, 1255 (1954). S. Asakura and F. Oosawa, *J. Polymer Sci.* 33, 183 (1958).
- [16] Y. N. Ohshima, H. Sakagami, K. Okumoto, A. Tokoyoda, T. Igarashi, K. B. Shintaku, S. Toride, H. Sekino, K. Kabuto and I. Nishio, *Phys. Rev. Lett.* 78, 3963 (1997).
- [17] Y. Mao, M. E. Cates and H. N. W. Lekkerkerker, *Physica A* 222, 10 (1995). P. Attard and G. N. Patey, *J. Chem. Phys.* 92, 4970 (1990). R. Dickman, P. Attard and V. Simonian, *J. Chem. Phys.* 107, 205 (1997). T. Biben, P. Bladon and D. Frenkel, *J. Phys.: Condens. Matter* 8, 10799 (1996).
- [18] J. P. Hansen, I. R. McDonald, *Theory of Simple Liquids* (Academic Press, London, 1986).